Photodissociation spectroscopy of Zn+(H2O) and Zn+(D2O)

Y. Abate and P. D. Kleiber

Citation: J. Chem. Phys. **122**, 084305 (2005); doi: 10.1063/1.1847610
View online: http://dx.doi.org/10.1063/1.1847610
View Table of Contents: http://jcp.aip.org/resource/1/JCPSA6/v122/i8
Published by the American Institute of Physics.

Photodissociation spectroscopy of $Zn^+(H_2O)$ and $Zn^+(D_2O)$

Y. Abate and P. D. Kleiber[a)]
Department of Physics and Astronomy, University of Iowa, Iowa City, Iowa 52242

(Received 21 October 2004; accepted 19 November 2004; published online 15 February 2005)

We report on a study of the photodissociation spectroscopy of weakly bound $Zn^+(H_2O)$ and $Zn^+(D_2O)$ complexes. The work is supported by *ab initio* electronic structure calculations of the ground and low-lying excited energy surfaces. We assign two molecular absorption bands in the near UV correlating to Zn^+ ($4s$-$4p$)-based transitions, and identify vibrational progressions associated with both intermolecular and intramolecular vibrational modes of the cluster. Partially resolved rotational structure is consistent with a C_{2V} equilibrium complex geometry. Experimental spectroscopic constants are in very good agreement with *ab initio* theoretical predictions. Results are compared with previous work on main group and transition metal ion-H_2O clusters.
 [DOI: 10.1063/1.1847610]

I. INTRODUCTION

There have been many spectroscopic studies of isolated gas phase metal ion-H_2O complexes, in part because of the importance of metal ion-H_2O interactions in solvation chemistry.[1–14] Several main group metal ions have been investigated[4–11] as well as some transition metal ions.[12–14] However, only a few cases have afforded rotational resolution allowing a direct spectroscopic determination of the equilibrium geometry of the complex.[4,5,11,14] The Duncan research group has studied the electronic spectroscopy of both Mg^+– and Ca^+–H_2O complexes, and verified the C_{2V} equilibrium geometry in each case.[4,5] Photodissociation spectroscopy through excited electronic states allows quantitative analysis of the geometry in both ground and excited states, giving valuable information about electronic structure and molecular orbital effects on the bonding interactions and reactivity. Using infrared photodissociation spectroscopic approaches it is possible to carry out direct spectroscopic studies of the ground state rovibrational structure for weakly bound clusters. For example, Vaden, Forinash, and Lisy have probed the rotational structure of $Cs^+(H_2O)Ar$.[11] More recently Walker *et al.* have investigated the infrared spectroscopy of $V^+(H_2O)Ar$ and found that the cluster distorts from a C_{2V} toward an insertionlike C_S geometry on excitation of the antisymmetric O–H stretch mode of the complex.[14]

Here we report results from a study of the UV-photodissociation spectroscopy of Zn^+–H_2O. Zn^+ is a transition metal ion with a valence structure, $Zn^+(3d^{10}4s^1)$, that is essentially similar to that of $Ca^+(4s^1)$. Despite this similarity in electronic character, in previous work we have often found significant differences in both the spectroscopy and chemical dynamics of analogous Ca^+- and Zn^+-molecule complexes.[15–17] These differences result in part from the relatively high ionization energy for Zn that opens charge transfer chemical channels at low excitation energies. For example, in both Mg^+–H_2CO and Ca^+–H_2CO, we have shown that the ground state equilibrium structure is C_{2V} with the metal ion bonded end-on to the O atom by primarily electrostatic ion-dipole forces.[15,16] However, for Zn^+–H_2CO, we have determined that the ground state equilibrium structure is C_S, bent with a Zn^+–O–C bond angle of $\sim 140°$.[17] This change in the bonding geometry results in part from a partial charge transfer in the ground state of the $Zn^+(H_2CO)$ complex. It is interesting to extend these studies to other Zn^+-molecule systems, including Zn^+–H_2O, to see how the equilibrium structure and bonding may differ from its main group metal ion counterparts. In addition, Zn^+ has a significantly larger spin-orbit coupling constant than Mg^+ or Ca^+, and it is interesting to see how the larger spin-orbit interaction may affect the spectroscopy and dissociation dynamics of the complex.

II. THEORETICAL CALCULATIONS

We have carried out a series of *ab initio* electronic structure calculations to investigate the bonding interactions in the ground and low-lying doublet excited states of $Zn^+(H_2O)$ using GAUSSIAN98.[18] Optimization calculations at the UHF/6-311++G($2d$,$2p$) (UHF—unrestricted Hartree–Fock) level find a ground state equilibrium for $Zn^+(H_2O)$ with Zn bonded end-on to the O atom in a C_{2V} complex similar to previous results for the analogous Mg^+- and Ca^+-water systems. The calculated Zn–O bond length is R(Zn–O)=2.092 Å at the UHF level, with a Zn–O bond dissociation energy of D_e''(Zn–O)=1.235 eV. Higher level UB3LPY/6-311++G($2d$,$2p$) density functional theory (DFT) calculations find essentially similar results but with a stronger Zn–O bond, R(Zn–O)=2.072 Å, and D_e''(Zn–O) =1.439 eV. The water ligand in the complex is relatively undistorted from its isolated geometry with an O–H bond length of R(O–H)=0.968 Å and H–O–H bond angle of $\angle$(HOH)=108.5° in the DFT calculation. Structural parameters and spectroscopic constants are summarized in Table I.

We have also used the UCIS/6-311++G($2d$,$2p$) (unrestricted configuration interaction-singles) method to study the low-lying doublet excited states of $Zn^+(H_2O)$. Calcula-

a)Author to whom correspondence should be addressed. Electronic mail: paul-kleiber@uiowa.edu

TABLE I. Structural parameters and spectroscopic constants for the low-lying states of $Zn^+(H_2O)$. Experimental results for $Zn^+(H_2O)$ are given in parentheses. All calculated results use a 6-311++G(2*d*,2*p*) basis.

	$1\ ^2A_1$		$1\ ^2B_2$	$1\ ^2B_1$
	UB31YP	UHF	UCIS	UCIS
R(ZnO) (Å)	2.072	2.092	1.945	1.982
R(OH) (Å)	0.968	0.947	0.947	0.947
∠(HOH)	108.5°	107.9°	110.2°	109.2°
A (cm^{-1})	13.6 (13.3±0.6)	14.3	13.9 (12.7±0.9)	14.0 (12.5±0.9)
$\frac{1}{2}(B+C)$ (cm^{-1})	0.26 (0.24±0.06)	0.25	0.29 (0.29±0.06)	0.28 (0.27±0.06)
$\omega_1(a_1)$ (cm^{-1})	3730	4041	4040	4040
$\omega_2(a_1)$	1640	1789	1784 (1577)	1792
$\omega_3(a_1)$	316	304	464 (523)	417 (491)
$\omega_4(b_2)$	3823	4126	4127	4121
$\omega_5(b_2)$	535	556	706 (700)	692 (675)
$\omega_6(b_1)$	78	321	326 (298)	357 (354)

tions show that the Zn^+-based $4p \leftarrow 4s$ transitions will dominate the UV absorption spectrum. We have found in several previous studies that the CIS method can work very well to describe the metal-centered excited states of a weakly bound complex. In $Zn^+(H_2O)$ there are three low-lying Zn^+*(4*p*)-based excited states $1\ ^2B_2(4p\pi)$, $1\ ^2B_1(4p\pi)$, and $2\ ^2A_1(4p\sigma)$, corresponding to states of different *p*-orbital alignment with respect to the intermolecular axis. The $4p\pi$ states are more strongly bound than the ground state and the corresponding Zn^+-based $4p\pi \leftarrow 4s\sigma$ absorption bands are significantly redshifted from the Zn^+ atomic resonance line at ~204 nm. In contrast, the $1\ ^2A_1(4p\sigma)$ state is less bound than the ground state and the corresponding absorption band is blueshifted beyond our spectrally accessible region. We have carried out UCIS optimization calculations for the $1\ ^2B_2(4p\pi)$ and $1\ ^2B_1(4p\pi)$ states. $1\ ^2B_2$ lies slightly lower in energy, with $T_e(1\ ^2B_2)=4.358$ eV and $T_e(1\ ^2B_1)=4.583$ eV. In each state the equilibrium geometry is C_{2V}, with a slight contraction in the Zn–O bond length and opening of the H–O–H bond angle. Excited state structural parameters and spectroscopic constants are also given in Table I.

III. EXPERIMENTAL ARRANGEMENT

The experimental approach has been described in earlier publications.[15,16,19] Weakly bound ion-molecule clusters, formed in a supersonic molecular beam apparatus equipped with a laser vaporization source are probed by photodissociation spectroscopy in an angular reflectron time-of-flight mass spectrometer (TOFMS). Based on an analysis of the spectral structure (*vide infra*) we estimate the rotational temperature of the clusters to be ~18 K. From the source, the molecular beam passes through a skimmer into a differentially pumped extraction chamber where ion clusters are pulse extracted, accelerated, and mass resolved in the first leg of the TOFMS. Parent ion clusters are mass selected with a pulsed mass gate and then focused into the reflectron region of the flight tube. Clusters are probed in UV with a tunable Nd:YAG (YAG–yttrium aluminum garnet) based OPO (optical parametric oscillator) system (Spectra Physics Pro-250 Nd:YAG pumped MOPO-SL) equipped with nonlinear frequency mixing capabilities. The laser bandwidth is ~0.15 cm^{-1}. Unreacted parent ions and daughter product ions are reaccelerated into the flight tube and mass resolved in the second leg of the TOFMS in a standard tandem time-of-flight arrangement. A microchannel plate detector is used to detect ions, and the signals are collected with a digital storage scope and gated integrator.

Photodissociation action spectra are determined by normalizing the mass-resolved daughter ion signal by the parent ion signal and laser power as a function of laser photon energy. The daughter ion signals are very weak in this experiment and so high laser powers are used to obtain a reasonable signal-to-noise ratio. As a result, observed bound-bound resonances are partially saturated and show some power broadening.

IV. EXPERIMENTAL RESULTS

The photodissociation action spectra for $Zn^+(H_2O)$ covers the near UV region from ~38 000 cm^{-1} to ~43 000 cm^{-1}. Zn^+ is the only daughter ion clearly observed although we cannot rule out that there may be some weak $ZnOH^+$ product signal that is unresolved from the large $Zn^+(H_2O)$ parent signal. Figures 1 and 2 show the photodissociation action spectra for $Zn^+(H_2O)$ and $Zn^+(D_2O)$, respectively. The action spectrum for $Zn^+(H_2O)$ is complex and shows a great deal of fine structure in the vibrational resonance progressions. The spectral complexity is due to a combination of rotational substructure, spin-orbit coupling, and overlapping vibrational and electronic band structure. The rotational structure (and some of the vibrational structure) in the $Zn^+(D_2O)$ case is not resolved making the spectrum appear much simpler.

The first group of resonance peaks in the $^{64}Zn^+(H_2O)$ spectrum of Fig. 1 appears at $T_{00}(1\ ^2B_2)=37\ 943\ cm^{-1}$, and we assign this structure to the $1\ ^2B_2 \leftarrow 1\ ^2A_1$ origin band. A careful search shows no evidence for any additional resonances to the red of this group of peaks, consistent with the assignment of this structure to the origin. This assumption is verified by isotopic substitution experiments using $^{66}Zn^+(H_2O)$, and making a pseudodiatomic approximation for the isotope shifts as discussed previously by Yeh *et al.*[20] Isotope shifts in the vibrational progression are consistent with this first observed structure being the origin band and not a higher vibrational level. The corresponding origin in $^{64}Zn^+(D_2O)$ is $T_{00}=37\ 936\ cm^{-1}$, and the small isotope shift for the band again supports the assignment.

From the origin of Fig. 1 there are at least four overlapping vibrational progressions with mode spacings of ~500 cm^{-1} building to higher energy. In the region near 40 300 cm^{-1} there is a marked increase in the spectral congestion. We identify the peak grouping at $T_{00}(1\ ^2B_1)=40\ 288\ cm^{-1}$ ($=0_0^0+2345\ cm^{-1}$) as the origin of the $1\ ^2B_1$

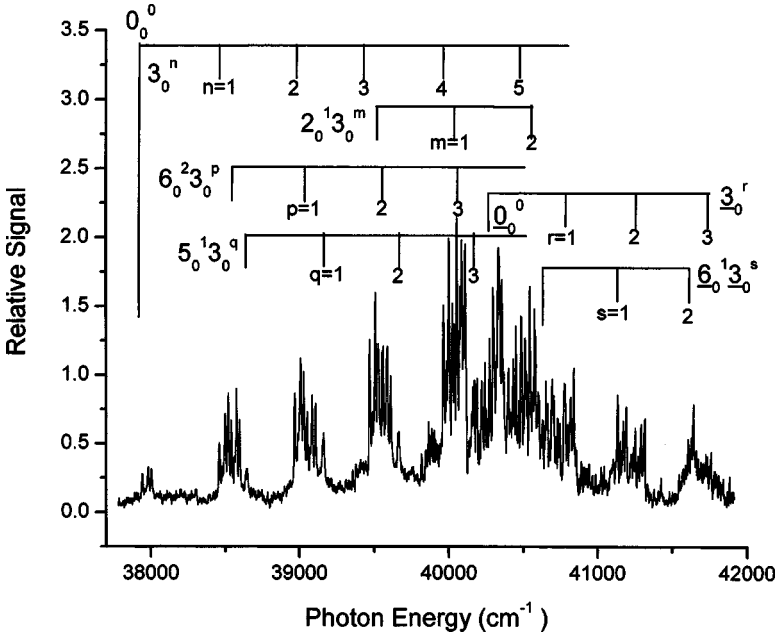

FIG. 1. Photodissociation action spectrum for $Zn^+(H_2O)$ showing the proposed vibronic assignment.

$\leftarrow 1\ ^2A_1$ band in $^{64}Zn^+(H_2O)$. The observed difference in B_2 and B_1 band origins, $\Delta E = 2345\ cm^{-1}$, is consistent with the CIS theoretical model results that predict a difference of $\Delta E = 1805\ cm^{-1}$ in the corresponding T_e values. The corresponding $1\ ^2B_1$ state origin in $^{64}Zn^+(D_2O)$ is at 40 289 cm^{-1}.

A. Rotational analysis of the $Zn^+(H_2O)$ origin bands

An expanded view of the $Zn^+(H_2O)$ $1\ ^2B_2$ band origin is shown in Fig. 3, and clearly exhibits rotational substructure with a multiplet of peaks. In the C_{2V} structure predicted by *ab initio* theory, the $Zn^+(H_2O)$ complex is well approximated as a prolate near symmetric top molecule. The $1\ ^2B_2 \leftarrow 1\ ^2A_1$ band is a perpendicular transition with the rotational selection rule $\Delta K = \pm 1$. At low rotational temperatures we expect three main peaks in the rotational substructure corresponding to the transitions $K'' = 0 \rightarrow K' = 1$ and $K'' = 1 \rightarrow K' = 0, 2$. However, the spin-orbit constant for Zn^+ is large and we must include the effect of spin-orbit interaction for a quantitative analysis of the rotational structure.

The combined effects of rotation-electronic and spin-orbit coupling have been discussed previously in work on weakly bound complexes $Ca(NH_2)$ and $Ca^+(H_2O)$.[6,21] These interactions have a significant quantitative and qualitative impact on the observed rotational structure, and the effects are even more pronounced in $Zn^+(H_2O)$ owing to the larger spin-orbit constant for Zn^+ [$A_{so}(Zn^+) = 583\ cm^{-1}$]. The effects can be understood following the discussion of Whitman and Jungen.[21] The interaction Hamiltonian is given approximately by

$$H_{int} = -2AN_aL_a + A_{so}L_aS_a,$$

where the first term describes the a-axis rotation-electronic (or Coriolis) coupling, and the second term gives the a-axis

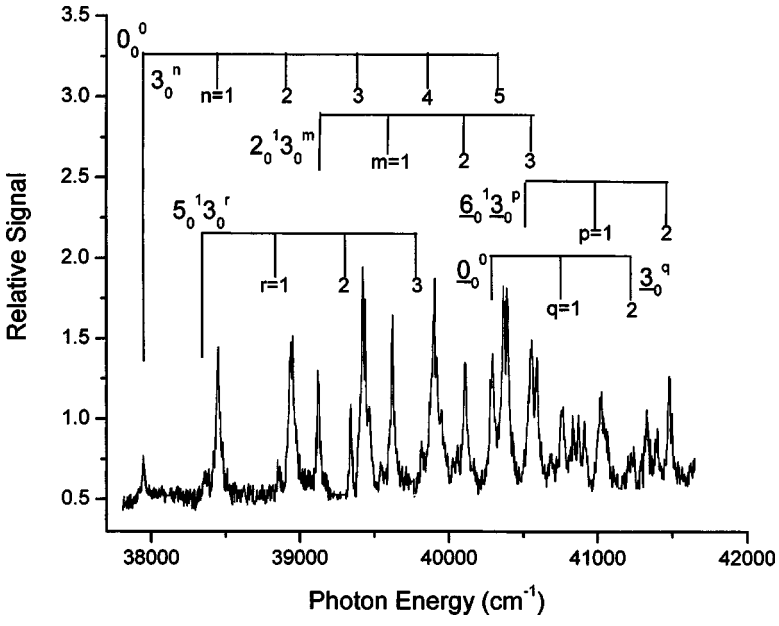

FIG. 2. Photodissociation action spectrum for $Zn^+(D_2O)$ showing the proposed vibronic assignment.

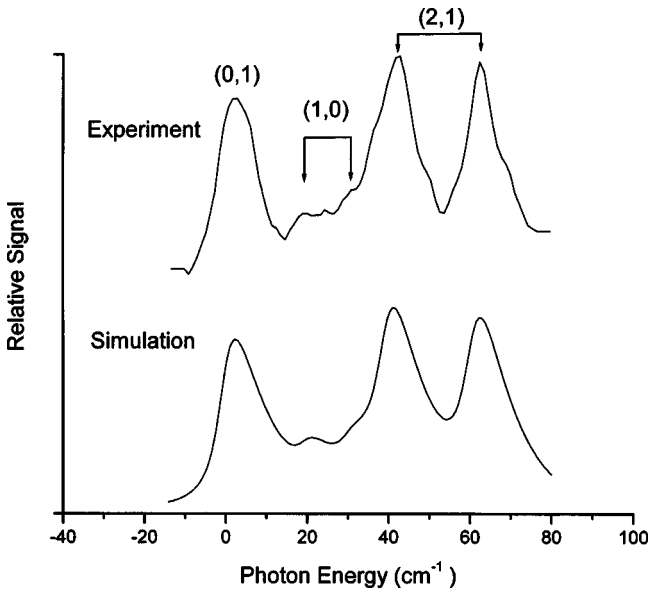

FIG. 3. Rotational structure for the $1\ ^2B_2$ state origin band in $Zn^+(H_2O)$. Spectroscopic constants determined from the simulation are given explicitly in Table I (in parentheses). Subband transitions (K'_a,K''_a) are indicated, and show the large spin splitting in the transitions for $K'_a>0$ as discussed in the text.

spin-orbit coupling. $1\ ^2B_2(\tilde{A})$ and $1\ ^2B_1(\tilde{B})$ represent electronic states with the Zn^+ $p\pi$ orbital aligned in the $Zn-OH_2$ plane and perpendicular to the plane, respectively. For nonzero K_a, the H_2 group rotates about the a axis, and for sufficiently fast rotation, the orbitals can decouple from the nuclear frame, resulting in a rotation induced mixing of the $\tilde{A}$ and $\tilde{B}$ states. This in turn induces a net electronic orbital angular momentum in each state that, through the combined effect of spin-orbit interaction, manifests itself as an anomalously large spin splitting in the rotational spectrum.

We follow the second-order perturbation theory treatment of Whitman and Jungen to quantitatively model the rotational substructure.[21] Essentially the analysis amounts to diagonalizing the 2×2 interaction Hamiltonian for the $\tilde{A}$ and $\tilde{B}$ state subspace. We assume a symmetric top model for the molecule $(B=\!=C)$ so that for the ground state, $1\ ^2A_1(\tilde{X})$ we have

$$E\left(\tilde{X};J=\!=N\pm\tfrac{1}{2},K\right)=B''N(N+1)+(A''-B'')K^2 \qquad (1)$$

while for the lowest two excited states, $1\ ^2B_2(\tilde{A})$ and $1\ ^2B_1(\tilde{B})$ we have,

$$E(\tilde{A};J,K)=T_0+A'(K^2+\Lambda^2)+B'J(J+1)+[A_{so}\Lambda^2\Sigma^2+4A'^2\Lambda^2K^2-4A_{so}A'\Lambda^2\Sigma K]/\Delta E \qquad (2)$$

and

$$E(\tilde{B};J,K)=T_0+A'(K^2+\Lambda^2)+B'J(J+1)-[A_{so}\Lambda^2\Sigma^2+4A'^2\Lambda^2K^2-4A_{so}A'\Lambda^2\Sigma K]/\Delta E, \qquad (3)$$

respectively.[21] In Eq. (1) we have neglected the small effect of the spin-rotation coupling (setting the spin-rotation coupling parameter equal to zero). In these results ΔE is the energy difference between the $1\ ^2B_2$ and $1\ ^2B_1$ band origins; we adopt the experimental value $\Delta E=2345\ cm^{-1}$. Λ and Σ are the usual orbital and spin angular momentum projections along the a axis, and here take on the values $\Lambda=1$ and $\Sigma=\pm\frac{1}{2}$. As discussed by Whitham and Jungen, the different spin projection values lead to a splitting of the rotational peaks for transitions with $K'\neq0$, due to the last term in the brackets of Eqs. (2) and (3), which is a cross term coupling rotation-electronic and spin-orbit effects.[21] The magnitude of the splitting depends on the molecular spin-orbit coupling strength, A_{so}. For Zn^+-based molecular complexes this value is large enough to split the expected three-peak spectrum effectively into a five-peak spectrum. (Although with our resolution, one of the peaks appears only as a weak shoulder on a larger peak.)

We have used eigenvalue Eqs. (1)–(3) to simulate the rotational spectrum for $Zn^+(H_2O)$. Essentially we sum contributions, weighted by the Hönl-London factors, for the allowed rovibronic transitions, and assuming a thermal population distribution in the ground state. Since we expect that ortho-para conversion should be negligible, we assume independent distributions for the K_a=even and K_a=odd states, with an ortho:para ratio fixed at 3:1. The electronic origin, rotational constants, and spin-orbit parameter are all then determined in the fitting procedure. The resulting model fit shown in Fig. 3 assumes a rotational temperature of 18 K and a Lorentzian bandwidth of $6\ cm^{-1}$, which is much greater than the laser linewidth of $\sim0.15\ cm^{-1}$, showing the combined effects of power broadening and lifetime broadening for the transitions. The best-fit spin-orbit constant in the $1\ ^2B_2$ state of $Zn^+(H_2O)$ is $A_{so}=490\ cm^{-1}$, which is ~0.84 times the $Zn^+(4p)$ atomic spin-orbit constant. This is in line with what may be expected based on previous work for $Ca^+(H_2O)$. The fitting was carried out for several data sets and the average best-fit values for the rotational constants are given in Table I (in parentheses).

The simulated fit to the data is excellent in both peak position and relative intensity. However, owing to the limited experimental resolution there are significant uncertainties in all of these values, although the differences in rotational constants $(A'-A''$ and $B'-B'')$ are known much more accurately than the individual values. In any case, there is excellent agreement between the experimental results and *ab initio* predictions (Table I). The major discrepancy lies in the predicted A-axis rotational constants where the HF and CIS methods overpredict the A constants by $\sim7\%$. In contrast, the ground state A constant at the DFT level is in very good agreement with the experimental value. The remarkably good overall agreement with theory gives compelling evidence to support the C_{2V} *ab initio* structure for the complex, in both ground and excited states.

There is ambiguity in converting the experimental spectroscopic constants into a molecular geometry, especially with the large uncertainties for individual rotational constants as shown in Table I. However, the experimental constants are consistent with the predicted geometry change on excitation including a shortening of the Zn–O bond and an increase in the HOH bond angle.

We have carried out a similar analysis for the $Zn^+(H_2O)$ $1\ ^2B_1$ state band origin and the results of the fitting procedure are similar. The fit is somewhat less reliable in this case because of an overlapping vibronic resonance from the $1\ ^2B_2 \leftarrow 1\ ^2A_1$ band. Nevertheless, the spin-orbit constant in the B_1 state is found to be $A_{so}=490\ cm^{-1}$, which is consistent with the value for the B_2 state as expected. Experimental rotational constants are again given in Table I.

B. Vibrational analysis of the $Zn^+(H_2O)$ bands

The observed vibrational resonances are listed explicitly in Table II. The characteristic rotational structure of the origin band is repeated in a long progression with a vibrational spacing of $\sim 500\ cm^{-1}$. This progression is assigned to the ν_3-Zn–O intermolecular stretch of a_1 symmetry (3_0^n). Birge-Sponer analysis of the stretch progression gives a mode frequency of $\omega_3(1\ ^2B_2)=523\ cm^{-1}$ and anharmonicity parameter $\omega_e x_e=3.8\ cm^{-1}$, in good agreement with the CIS predicted frequency of $464\ cm^{-1}$ for this mode.

The stretch progression is repeated several times in combination bands with other modes in the spectrum. A glance at the first grouping of peaks above the origin near $38\ 500\ cm^{-1}$ shows evidence for two additional active vibrational modes. In addition to the rotational multiplet structure that corresponds to one quantum of intermolecular stretch at $\sim 38\ 458\ cm^{-1}$, 3_0^1, there is obviously a second and very similar multiplet structure at slightly higher energy, and at higher energy yet, a broader singlet peak. These additional vibrational modes are too low in energy to be intramolecular water vibrations, and must correspond to intermolecular bending modes of the complex.

We can use the characteristic rotational structure to assign the modes. The singlet peak at $38\ 643\ cm^{-1}$ ($=0_0^0 + 700\ cm^{-1}$) is assigned to one quantum of the in-plane ν_5-intermolecular bend of b_2 symmetry (5_0^1). The overall vibronic species is $b_2 \times b_2 = a_1$, corresponding to a parallel transition with selection rule $\Delta K=0$, and leading to a single major absorption peak with unresolved rotational state substructure. The fundamental frequency is then $\omega_5(1\ ^2B_2) = 700\ cm^{-1}$, which is in very good agreement with the CIS predicted frequency of $706\ cm^{-1}$ for this mode.

The second multiplet of peaks in the grouping near $38\ 539\ cm^{-1}$ ($=0_0^0 + 596\ cm^{-1}$) can be assigned to the second quantum of the ν_6 out-of-plane intermolecular bend of b_1 symmetry. This mode is forbidden in a single quantum with overall vibronic species $b_2 \times b_1 = a_2$, but allowed in the second quantum (6_0^2) with overall species $b_2 \times b_1 \times b_1 = b_2$. Excitation of the second quantum is allowed in a perpendicular transition, showing a triplet rotational structure. Normally this transition would be expected to be very weak; however, here the band can borrow intensity by mixing with the near resonant 3_0^1 state of the same overall symmetry. The fundamental mode energy is then $\omega_6(1\ ^2B_2)=596/2=298\ cm^{-1}$, in fairly good agreement with the CIS predicted value of $326\ cm^{-1}$ for this mode.

Each of these intermolecular modes forms the basis for a progression in the combination bands $5_0^1 3_0^n$ and $6_0^2 3_0^n$ as shown in Fig. 1 and given explicitly in Table II. We have also identified one more combination mode at higher frequencies, $2_0^1 3_0^n$, the combination of the ν_2-symmetric HOH bend of a_1 symmetry and the intermolecular stretch. This band gives an overlapping progression of multiplets built on an origin at $39\ 520\ cm^{-1}$. The corresponding mode frequency $\omega_2(1\ ^2B_2) = 1577\ cm^{-1}$ is in fair agreement with the CIS predicted value of $1784\ cm^{-1}$.

The spectrum becomes more congested with the onset of the $1\ ^2B_1 \leftarrow 1\ ^2A_1$ band origin at $T_{00}=40\ 288\ cm^{-1}$, making a

TABLE II. Observed resonances and vibrational assignments for $Zn^+(H_2O)$ and $Zn^+(D_2O)$ in $1\ ^2B_2$ and $1\ ^2B_1$. The modes assigned to $1\ ^2B_1$ are underlined. In every case the lower state is assumed to be the vibrationless ground state.

$Zn^+(H_2O)$	
Resonance	Assignment
37 943	0^0
38 458	3^1
38 539	6^2
38 643	5^1
38 967	3^2
39 051	$6^2\ 3^1$
39 158	$5^1\ 3^1$
39 468	3^3
39 520	2^1
39 555	$6^2\ 3^2$
39 664	$5^1\ 3^2$
39 960	3^4
40 033	$2^1\ 3^1$
40 049	$6^2\ 3^3$
40 161	$5^1\ 3^3$
40 288	$\underline{0}^0$
40 446	3^5
40 539	$2^1\ 3^2$
40 642	$\underline{6}^1$
40 773	$\underline{3}^1$
41 128	$\underline{6}^1\ \underline{3}^2$
41 249	$\underline{3}^2$
41 601	$\underline{6}^1\ \underline{3}^2$
41 638	$\underline{5}^2$
41 721	$\underline{3}^3$
$Zn^+(D_2O)$	
37 936	0^0
38 370	5^1
38 448	3^1
38 860	$5^1\ 3^1$
38 938	3^2
39 118	2^1
39 339	$5^1\ 3^2$
39 420	3^3
39 620	$2^1\ 3^1$
39 814	$5^1\ 3^3$
39 897	3^4
40 103	$2^1\ 3^2$
40 289	$\underline{0}^0$
40 363	3^5
40 580	$2^1\ 3^3$
40 552	$\underline{6}^1$
40 826	3^6
41 014	$\underline{6}^1\ \underline{3}^1$
41 473	$\underline{6}^1\ \underline{3}^2$

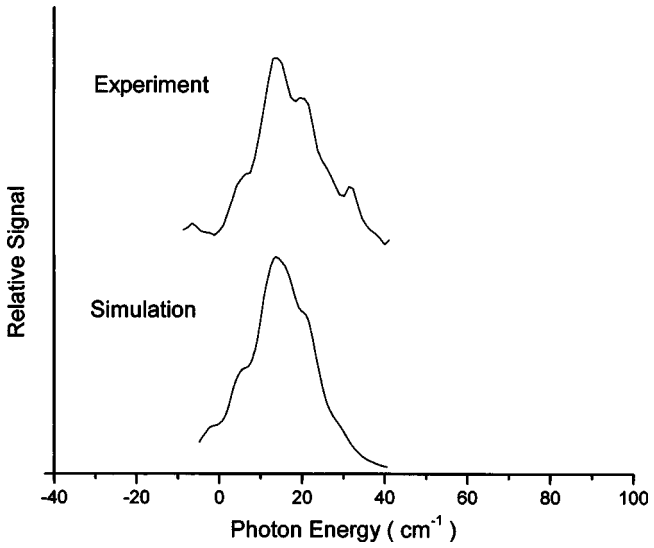

FIG. 4. Rotational structure for the $1\ ^2B_2$ state origin band in $Zn^+(D_2O)$. Spectroscopic constants determined from the simulation are $A''=3.6\ cm^{-1}$, $\frac{1}{2}(B''+C'')=0.25\ cm^{-1}$, $A'=3.5\ cm^{-1}$, $\frac{1}{2}(B'+C')=0.30\ cm^{-1}$, and $A_{so}=391\ cm^{-1}$, with an ortho:para ratio of 1:2.

detailed assignment at higher energies difficult. However, we can clearly identify the intermolecular stretch progression in the $1\ ^2B_1$ state with a vibrational frequency of $C_3(1\ ^2B_1)=485\ cm^{-1}$. We have also tentatively identified two members of the $6_0^1 3_0^n$ combination band in $1\ ^2B_1$ as shown in Fig. 1 and listed in Table II. In the $^2B_1$ electronic excited state, the v_6-out-of-plane intermolecular bending mode of the complex has b_1 symmetry and is allowed in one quantum with a parallel type polarization band contour. The observed fundamental frequency for this mode is $\omega_6(1\ ^2B_1)=354\ cm^{-1}$ in excellent agreement with CIS prediction of $357\ cm^{-1}$ for this mode. We have also tentatively identified the second quantum of the v_5 in-plane intermolecular bending vibration (5_0^2) in the $1\ ^2B_1$ state as shown in Fig. 1 and given explicitly in Table II. This IP bending mode has b_2 symmetry, so the first quantum is not allowed. However two quanta of this mode will be allowed with overall b_2 resonance at character, giving rise to a transition with a perpendicular type band contour. The fundamental frequency for this mode is then determined experimentally to be $\omega_5(1\ ^2B_1)=1350/2=675\ cm^{-1}$, in very good agreement with CIS prediction of $692\ cm^{-1}$.

C. Comparison with $Zn^+(D_2O)$

To validate the spectral assignments we have also carried out experiments on the $^{64}Zn^+(D_2O)$ isotopomer. The action spectrum and vibrational assignment are shown in Fig. 2. The corresponding $1\ ^2B_2$ state origin in $^{64}Zn^+(D_2O)$ is at $T_{00}=37\ 936\ cm^{-1}$. We have carried out a rotational analysis of the origin band and the results are shown in Fig. 4. In this case the smaller rotational constants and limited spectral resolution makes it difficult to obtain quantitative values for the spectroscopic constants. The best-fit spectroscopic constants for the $1\ ^2A_1$ and $1\ ^2B_2$ states of $Zn^+(D_2O)$ are $A''=3.6\ cm^{-1}$, $\frac{1}{2}(B''+C'')=0.25\ cm^{-1}$, $A'=3.5\ cm^{-1}$, $\frac{1}{2}(B'+C')=0.30\ cm^{-1}$, and $A_{so}=391\ cm^{-1}$.

Analysis of the isotope shifts in the vibrational spectrum is also informative. The vibrational spectrum of $Zn^+(D_2O)$ appears much simpler. This is due in part to the fact that the rotational substructure is largely unresolved. The intermolecular stretch progression in $1\ ^2B_2$, 3_0^n can be readily identified. Birge-Sponer analysis gives the fundamental frequency of $\omega_3^D(1\ ^2B_2)=513\ cm^{-1}$ with an anharmonicity of $\omega_e x_e=4.6\ cm^{-1}$. The isotope shift $\omega_3(Zn-D_2O)/\omega_3(Zn-H_2O)=0.98$ is in excellent agreement with the expected value based on the pseudodiatomic approximation (0.96) (and with the expected value from the CIS calculations).

The combination band progression for $Zn^+(D_2O)$, $5_0^1 3_0^n$ is observed as a series of singlet peaks on the low energy side of the main stretch progression. The fundamental v_5 in-plane bending mode frequency is $\omega_5^D(1\ ^2B_2)=434\ cm^{-1}$. The isotope shift, $\omega_5(Zn-D_2O)/\omega_5(Zn-H_2O)=0.62$ is consistent with the *ab initio* predicted isotope shift of 0.74 for this mode. The combination band progression, $2_0^1 3_0^n$, can also be readily identified in the spectrum. The observed fundamental frequency for the v_2-HOH symmetric bend in $Zn^+(D_2O)$ is $\omega_2^D(1\ ^2B_2)=1182\ cm^{-1}$. Again, the isotope shift $\omega_2(Zn-D_2O)/\omega_2(Zn-H_2O)=0.75$ is in good agreement with the *ab initio* predicted isotope shift for this mode of 0.74.

The expected combination band $6_0^2 3_0^n$ is not readily apparent in the $Zn^+(D_2O)$ spectrum. However, based on the isotope shift predicted by *ab initio* theory for this band, we would expect the first observed peak in the band to lie at $6_0^2=454\ cm^{-1}$, which is very nearly resonant with 3_0^1. Thus, it appears that the 3_0^n and $6_0^2 3_0^n$ progressions in $Zn^+(D_2O)$ are unresolved in our spectrum. Indeed, the resonance peaks in the stretch progression are appreciably broader than the origin band and, each member shows evidence for a shoulder on the high-energy side, consistent with two very near resonant overlapping progressions.

The $1\ ^2B_1$ state origin in $Zn^+(D_2O)$ is found at 40 289 $(=0_0^0+2353)\ cm^{-1}$. We can again clearly identify the Zn–O intermolecular stretch mode in the B_1 state with an observed frequency of $\omega_3^D(1\ ^2B_1)=467\ cm^{-1}$. We can also identify two members of the combination band progression $6_0^1 3_0^n$ in the $Zn^+(D_2O)$ $1\ ^2B_1 \leftarrow 1\ ^2A_1$ spectrum as shown in Fig. 2. The observed fundamental frequency for this mode is $\omega_6^D(1\ ^2B_1)=263\ cm^{-1}$, in excellent agreement with CIS prediction of $272\ cm^{-1}$. The isotope shifts for each of these assigned modes are again in very good agreement with the *ab initio* predicted isotope shifts.

With these H–D isotope substitution experiments we can identify and assign all of the major spectral features, and the good agreement with predicted isotope shifts for all of the features is strong evidence to support our spectral assignment.

V. SUMMARY

The excellent agreement between the experimental and *ab initio* theory spectroscopic constants gives strong support for the theoretical predictions for complex structure and bonding. The transition metal complex, $Zn^+(H_2O)$ has C_{2v} symmetry in both ground and excited states. The agreement for both rotational constants and excited state vibrational fre-

quencies is remarkably good even for a relatively low level HF/CIS based calculation. Note, also that the intermolecular frequencies tend to be well predicted at the CIS level, without the 90% scaling rule that is commonly applied to higher energy intramolecular vibrational frequencies.

Our results are in good accord with the earlier results from a study of $Ca^+(H_2O)$ results by the Duncan group, showing that the spectroscopy and bonding of the $Zn^+(H_2O)$ and $Ca^+(H_2O)$ complexes are quite similar. This is somewhat surprising given the dramatic differences between Zn^+-molecule and Ca^+-molecule clusters we have often seen previously. The main point appears to be that the IE for H_2O is itself quite high, so that charge transfer interactions play a very minor role in the $Zn^+(H_2O)$ case.

Finally, it is important to note that accurate modeling of the rotational multiplet structure requires a careful treatment of spin-orbit interactions. The second-order perturbation theory treatment by Whitham and Jungen[21] works very well, even for this case with a very large spin-orbit coupling constant.

ACKNOWLEDGMENTS

This research was supported by the National Science Foundation under Grant No. CHE-9982119. The authors gratefully acknowledge helpful discussions with Professor Dennis Clouthier.

[1] J. M. Lisy, Int. Rev. Phys. Chem. **16**, 267 (1997).
[2] K. Fuke, K. Hashimoto, and S. Iwata, Adv. Chem. Phys. **110**, 431 (1999).
[3] J. M. Farrar, Int. Rev. Phys. Chem. **22**, 593 (2003).
[4] K. F. Willey, C. S. Yeh, D. L. Robbins, J. S. Pilgrim, and M. A. Duncan, J. Chem. Phys. **97**, 8886 (1992).
[5] C. T. Scurlock, S. H. Pullins, J. E. Reddic, and M. A. Duncan, J. Chem. Phys. **104**, 4591 (1996).
[6] F. Misaizu, M. Sanekata, K. Tsukamoto, K. Fuke, and S. Iwata, J. Phys. Chem. **96**, 8259 (1992).
[7] F. Misaizu, M. Sanekata, K. Fuke, and S. Iwata, J. Chem. Phys. **100**, 1161 (1994).
[8] M. Sanekata, F. Misaizu, and K. Fuke, J. Chem. Phys. **104**, 9768 (1996).
[9] C. J. Weinheimer and J. M. Lisy, J. Chem. Phys. **105**, 2938 (1996).
[10] D. C. Sperry, A. J. Midey, J. I. Lee, J. Qian, and J. M. Farrar, J. Chem. Phys. **111**, 8469 (1999).
[11] T. D. Vaden, B. Forinash, and J. M. Lisy, J. Chem. Phys. **117**, 4628 (2002).
[12] D. E. Lessen, R. L. Asher, and P. J. Brucat, J. Chem. Phys. **93**, 6102 (1990).
[13] L. Dukan, L. del Fabbro, P. Pradel, O. Sublemontier, J. M. Mestdagh, and J. P. Visticot, Eur. Phys. J. D **3**, 257 (1998).
[14] N. R. Walker, R. S. Walters, E. D. Pillai, and M. A. Duncan, J. Chem. Phys. **119**, 10471 (2003).
[15] W.-Y. Lu, T. H. Wong, Y. Sheng, and P. D. Kleiber, J. Chem. Phys. **117**, 6970 (2002).
[16] W.-Y. Lu, T. H. Wong, Y. Sheng, and P. D. Kleiber J. Chem. Phys. **118**, 6905 (2003).
[17] W.-Y. Lu, Y. Abate, T.-H. Wong, and P. D. Kleiber, Knowledge Inf. Syst. **108**, 10661 (2004).
[18] M. J. Frisch, G. W. Trucks, H. B. Schlegel *et al.*, GAUSSIAN 98, Revision A6, Gaussian Inc., Pittsburgh, PA, 1998.
[19] P. D. Kleiber and J. Chen, Int. Rev. Phys. Chem. **17**, 1 (1998).
[20] C. S. Yeh, K. F. Willey, D. L. Robbins, and M. A. Duncan, J. Chem. Phys. **98**, 1867 (1993).
[21] C. J. Whitham and Ch. Jungen, J. Chem. Phys. **93**, 1001 (1990).